Applied Surface Science Advances 5 (2021) 100120

Contents lists available at ScienceDirect

Applied Surface Science Advances

journal homepage: www.sciencedirect.com/journal/applied-surface-science-advances

Plasticized I_2-free polysiloxane ionic conductors as electrolytes for stable and flexible solid-state dye-sensitized solar cells

Anil Kumar Bharwal [a,b,*], Girish D. Salian [c], Laura Manceriu [a], Abdelfattah Mahmoud [a], Fannie Alloin [b], Cristina Iojoiu [b], Thierry Djenizian [c,d], Carmen M. Ruiz [e], Marcel Pasquinelli [e], Thierry Toupance [f], Celine Olivier [f], David Duché [e], Jean-Jacques Simon [e], Catherine Henrist [a,*]

[a] University of Liège, CESAM-GREEN-MAT, Allée du Six-Aout 13, 4000 Liège (Sart Tilman), Belgium
[b] Univ. Grenoble Alpes, Univ. Savoie Mont Blanc, CNRS, Grenoble INP, LEPMI, 38000 Grenoble, France
[c] Mines Saint-Etienne, Center of Microelectronics in Provence, Department of Flexible Electronics, F – 13541 Gardanne, France
[d] Al-Farabi Kazakh National University, Center of Physical-Chemical Methods of Research and Analysis, Tole bi str., 96A. Almaty, Kazakhstan
[e] Aix-Marseille Univ., Univ. Toulon, UMR CNRS 7334, IM2NP, Marseille, France
[f] Université de Bordeaux, Institut des Sciences Moléculaires, ISM UMR 5255 CNRS, 351 Cours de la Libération, F-33405 Talence, Cédex, France

ARTICLE INFO

Keywords:
I_2-free polymer electrolytes
Visible light absorption
TiO_2 nanotubes
Electron lifetime

ABSTRACT

For practical applications, flexible solid-state dye-sensitized solar cells (ss-DSSCs) with high photovoltaic performance and stability are paramount. A novel iodine (I_2)-free polysiloxane based highly conductive poly(ionic liquid), which acts as the lone charge transfer intermediate, is used for the first time as an electrolyte in flexible 1D TiO_2 nanotube photoanodes (TiO_2 NT) based ss-DSSCs. The I_2-free polymer electrolyte plasticized with ethylene carbonate (EC) leads to a higher power conversion efficiency in DSSCs involving TiO_2 NTs than the I_2-based polymer electrolyte, mainly due to improved V_{oc} and J_{sc}. Apart from overcoming the visible light absorption loss, this I_2-free polymer electrolyte also reduces the charge recombination and thus leads to higher electron lifetime in DSSCs. The I_2-free DSSCs also displayed long-term stability measured under ambient and accelerated stability testing. The improvement is also due to the effective pore infiltration into the large pores of TiO_2 NT structure in ss-DSSCs.

1. Introduction

Over the years, the photovoltaic technologies have emerged as an attractive alternative energy source to fossil fuels because of the constant solar energy supply by the sun [1]. Since last two decades, dye-sensitized solar cells (DSSCs) have been given noteworthy attention due to their low manufacturing cost, easy fabrication, high power conversion efficiency (PCE), aesthetics as well as for their environment friendly nature [2–6]. Usually, a DSSC consists of four major components: photoanode, dye, redox electrolyte, and counter electrode. Optimization of all components is equally essential for performance improvement of DSSCs. In particular, the electrolyte is a key component in DSSCs, as it has to be an effective redox mediator and show long-term stability. Kakiage et al. reported groundbreaking PCEs over 14% for DSSCs containing Co^{2+}/Co^{3+} redox liquid electrolytes [7]. However, DSSCs consisted of liquid electrolyte possess stability related issues due to electrolyte leakage. To overcome the drawbacks related to stability, a large number of solid-state and quasi solid-state electrolytes, such as organic hole-transporting materials [8], conducting polymer [9], copper iodide or thiocyanate [10], ionic liquids (ILs) [11,12] as well as poly (ionic liquid)s (PILs) based electrolytes [13–18] have been studied as alternatives to the liquid electrolytes. An impressive PCEs of 11.7% was reported for ss-DSSCs with solid copper-based electrolyte [19]. However, polymer electrolytes based on PILs are preferred over inorganic solid electrolytes owing to their flexible nature and similar working mechanism as liquid electrolytes [20–23]. Pang et al. developed quasi-solid state electrolyte by soaking poly(vinylidene fluoride-co-hexafluoropropylene) (PVDF-HFP) based PILs into liquid electrolytes and the resulting DSSCs showed improved durability [21]. Recently, a novel multifunctional PIL, poly(oxyethylene)-imide-2,2,6,6-tetramethyl-1-piperidinyloxy was used as additive in liquid electrolyte and the resulting DSSCs maintained the long-term stability and PCE [24].

Polysiloxane-based electrolytes have been used in DSSCs due to their

* Corresponding authors.
E-mail addresses: anilkumar.bharwal@alumni.uliege.be (A.K. Bharwal), catherine.henrist@uliege.be (C. Henrist).

https://doi.org/10.1016/j.apsadv.2021.100120
Received 16 February 2021; Received in revised form 26 May 2021; Accepted 7 June 2021
Available online 22 June 2021

excellent properties such as highly flexible and hydrophobic backbone, low T_g, and robust nature [25–27]. In our previous studies, we demonstrated the long-term stability for polysiloxane electrolytes based DSSCs [28–30]. However, all these polymer electrolytes still contained iodine (I_2), which is known to cause the formation of extra I_3^- ions leading to photodegradation, corrosion of the counter electrode and desorption of the dye and thus limited stability. In 2011, Wang et al. reported the use of an I_2-free PIL, poly(1-alkyl-3-(acryloyloxy) hexylimidazolium, as solid- state electrolyte in DSSC and achieved a PCE of 5.3%, retaining 85% of its original PCE after 1000 h at room temperature [31]. Yu et al. reported quasi-solid state DSSCs based on electrolytes gelled with 15 wt.% TiO_2 and achieved a PCE of 8.0% [32]. Besides, some reports dealt with DSSCs with I_2-free DSSC, showing reasonable performances, but only scarcely detailed their stability [33–36].

On the basis of these works about I_2-free DSSCs, we herein report for the first time the use of a I_2-free poly(1-N-methylimidazolium-pentylpolydimethylsiloxane)iodide as PIL in DSSCs including photoanodes made of TiO_2 nanotubes (TiO_2 NTs) immobilized on flexible Ti-foil. Indeed, due to their polymeric nature, polysiloxane-based PILs are viscous and a poor infiltration into TiO_2 mesoporous structures was noticed [29]. The one-dimensional (1D) structured TiO_2 NTs improves the polymer electrolyte infiltration into the photoanode as well as the charge transport [37–42]. Seidalilir et al. [43] reported gel-state DSSCs based on TiO_2 NTs photoanodes with a PCE of 7.1%, the improved PCE being attributed to the effective pore infiltration and continuous electrons transfer. In this work, we combine a flexible 1D TiO_2 NT photoanode and polysiloxane based I_2-free PIL electrolyte, to develop efficient and stable DSSC devices. The device performances were investigated by measuring current density-voltage (*J-V*) curves, dark current, impedance spectroscopy (EIS) and open-circuit voltage decay (OCVD).

2. Experimental

2.1. Preparation of 1D TiO_2 nanotubes (TiO_2 NTs) based photoanodes

The TiO_2 NTs were fabricated by the electrochemical anodization of the Ti foil. The cut Ti foil of 2 cm × 2 cm dimension was cleaned and sonicated in acetone, isopropanol and methanol sequentially for 10 min each and then dried in compressed air. Anodization of the cleaned Ti foil was performed in an electrolyte solution containing 0.3 M NH_4F and 5% v/v water in ethylene glycol, by applying a constant voltage of 60 V between the Ti foil and a Pt foil counter electrode for 1 h using a generator (ISO-TECH IPS-603). The amorphous TiO_2 NTs obtained after anodization were gently sonicated in deionized (DI) water to remove the nanograss (hydroxide) formation on the nanotubes. The amorphous sample was washed in DI water and dried with compressed air. To obtain the anatase phase, the amorphous TiO_2 NTs were annealed in air at 450 °C for 3 h.

2.2. Preparation of the polymer electrolyte

The PIL, poly(1-N-methylimidazolium-pentylpolydimethylsiloxane) iodide (referred to "ImI-PDMS" in this article) was synthesized as reported in our previous work (see supporting information) [25]. Fig. S1 show the chemical structures of ImI-PDMS and ethylene carbonate (EC). The polymer electrolytes composition used in this work is displayed in the Table S1. Appropriate amounts of the components were dissolved in a small amount of acetonitrile/valeronitrile (85/15, vol/vol) in a closed bottle and then continuously stirred at 50 °C for 5 mins. The experimental procedure for fabricating DSSCs devices by using TiO_2 NTs and electrolytes and the characterization techniques are detailed in the Supporting Information.

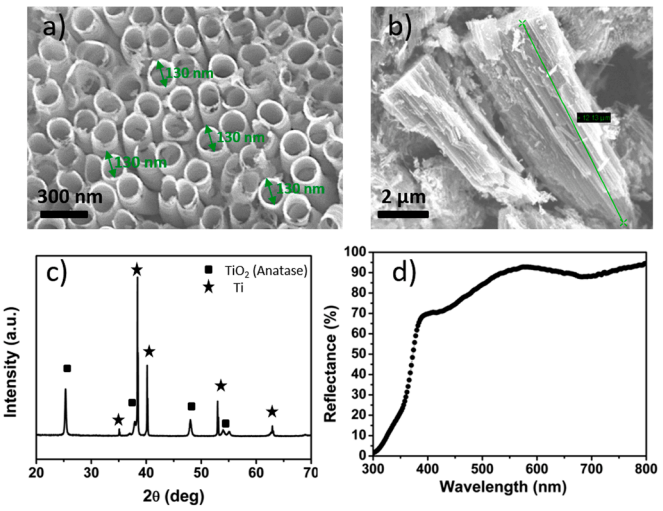

Fig. 1. SEM images displaying the top view (a), and side-view (b), of the TiO_2 NTs array grown by anodization of Ti foil. In (c), the XRD pattern of the calcined TiO_2 NTs grown on Ti foil, while panel (d) shows the diffusive reflectance spectra of the TiO_2 NTs.

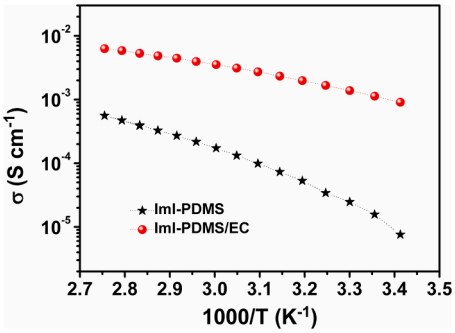

Fig. 2. The temperature dependence of the ionic conductivity of ImI-PDMS with and without EC.

3. Results and discussion

3.1. Morphological and structural analysis of 1D TiO_2 NTs

Fig. 1a and b show the SEM images of the TiO_2 NTs arrays, exhibiting an inner diameter ~ 130 nm and ~ 12 µm length. The unidirectional vertical arrangement of the nanotubes permits faster electron transfer in comparison to a dense nanoparticles network [43]. The structure of the grown TiO_2 NTs was determined by XRD, as shown in Fig. 1c. All the TiO_2 NTs layers present the anatase phase structure (JCPDS 89–4921) with main diffraction lines which can be indexed as the (101), (004),

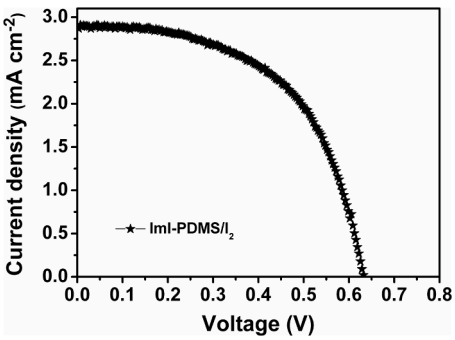

Fig. 3. *J-V* curves of the device using ImI-PDMS/I_2.

Table 1
Photovoltaic parameters of DSSCs based on Dyesol TiO_2 or TiO_2 NTs photoanodes in contact with ImI-PDMS/I_2 electrolyte.

Photoanodes	Thickness (μm)	Illumination	Dye loading (mol mm^{-2})	Sun (mW cm^{-1})	J_{sc} (mA cm^{-2})	V_{oc} (V)	FF	PCE (%)	Ref
Dyesol TiO_2	11	Front	1.98×10^{-9}	0.7	5.9	0.11	0.25	0.2	[29]
TiO_2 NTs	12	Back	7.0×10^{-12}	0.6	2.9	0.63	0.55	1.7	present work

(200) and (105) crystal planes, while the extra peaks come from the metallic Ti foil. Also, the sharp diffraction peaks in Fig. 1c. reveal that the TiO_2 NT is characterized by a high crystallinity, which is related to the high-temperature post-deposition treatment at 450 °C under air. It has been reported that light scattering of TiO_2 photoanode in DSSCs is useful in improving light harvesting properties [44–47]. Fig. 1d represents the diffuse reflectance spectra indicating that the TiO_2 NTs also have the capacity to improve light harvesting in DSSCs. Fig. S2 illustrates digital photographs of the unfolded Ti foil with dye-absorbed TiO_2 NTs and the same bended sample confirming the flexible nature of the photoanode.

3.2. Properties of the polymer electrolyte

ImI-PDMS is a PIL composed of imidazolium cations fixed on a polysiloxane backbone using a pentyl spacer. The ionic conductivity of ImI-PDMS electrolyte is found to be 1.6×10^{-5} S cm^{-1} at room temperature. Upon plasticizing with 33 wt.% of EC, the conductivity is enhanced to 1.1×10^{-3} S cm^{-1}. The large increment in conductivity is attributed to the lower viscosity and a surge in ion dissociation because of the huge dielectric constant of EC. As shown in Fig. 2, the ionic conductivity increases with temperature increase.

3.3. Photovoltaic performance of the polymer electrolyte

Fig. 3 shows the *J-V* curves of the DSSCs based of flexible Ti-foil-based TiO_2 NTs and the pure ImI-PDMS/I_2 electrolyte measured under ~ 0.6 sun illumination, while the Table 1 lists the photovoltaic performance parameters. The device composed of ImI-PDMS/I_2 as electrolyte and TiO_2 NTs photoanode, yielded higher J_{sc} (2.9 mA cm^{-2}) and PCE (1.7%) than the one reported in our previous study using TiO_2 dyesol as photoanode with a similar thickness [29]. Despite having significantly lower dye loading, the enhanced performance is coming from the improved pore infiltration of the ImI-PDMS/I_2 electrolyte inside the TiO_2 NT pores as shown in Fig. 4. After polymer infiltration, the individual TiO_2 NTs cannot be differentiated as polymer has infiltrated throughout the entire film. Furthermore, EDX elemental analysis confirmed the presence of Si, C and I atoms across the 12 μm thick TiO_2 NP film (Fig. 4b). Additionally, higher scattering properties of TiO_2 NT compromise the loss occurred due to lower dye loading (Fig. 1d).

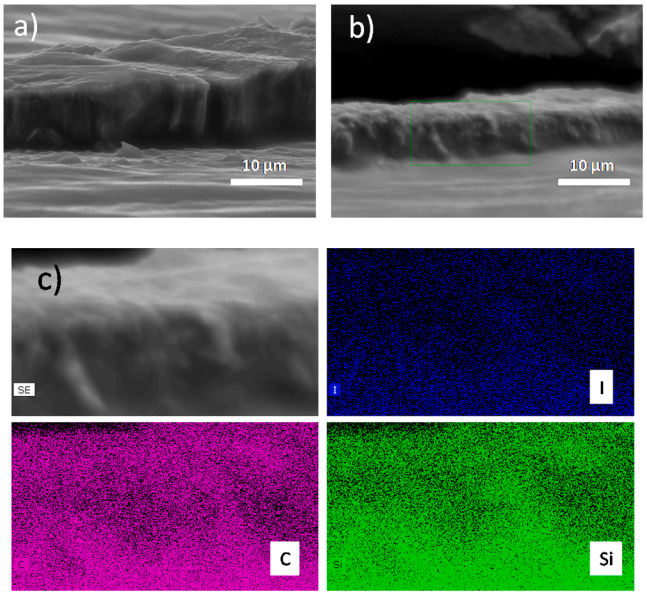

Fig. 4. SEM cross-section images of the TiO_2 NTs filled with ImI-PDMS/I_2 (a) and (c) EDX elemental mapping for the rectangular area indicated in (b).

Fig. 5a and Table 2 show the photovoltaic parameters of the DSSCs comprised of reference (liquid electrolyte) and polymer electrolytes under ~ 0.6 sun illumination. The device based on the liquid electrolyte showed the highest PCE of 4.15% as compared to the one with polymer electrolytes, which is mainly due to higher ionic conductivity and diffusion coefficient of I_3^- ions in the liquid electrolyte [28–30]. It is worth noting that the addition of 33 wt.% EC into the ImI-PDMS/EC/I_2 polymer electrolytes results in an improvement of both V_{oc} and J_{sc}, resulting in a PCE of 2.3% (Tables 1 and 2). Interestingly, the PCE reached 3.55%, when I_2 was omitted from the polymer electrolyte exhibiting a maximum IPCE value of 38.5% at 530 nm (Fig. S3). The omission of I_2 improved the J_{sc} and V_{oc}, with a negligible impact on FF. The FF is the ratio of maximum attainable power to the product of J_{sc} and V_{oc}. Therefore, its reduction is probably due to enhanced charge transport resistance resulting from a lower I_3^- concentration generated in-situ in I_2-free electrolyte [48]. The improved V_{oc} and J_{sc} can be correlated to the reduced dark current as shown in Fig 5b.

Our study shows that it is not necessary to add I_2 in polysiloxane based PIL and is even detrimental (Table 2 and Fig 5). The addition of extra I_2 engenders the in-situ generation of excess I_3^- which could further develop into polyiodides such as I_5^- and I_7^- [49]. The visible light absorption spectra of ImI-PDMS/EC/I_2 and ImI-PDMS/EC (both 10x diluted with acetonitrile/valeronitrile) indicated that the I_2-free electrolyte absorbs less visible light compared to the one with I_2 (Fig. 6a). Furthermore, removal of I_2 from the polymer electrolytes makes the electrolyte lighter in color and improves the light-harvesting of the dye molecules (insert of Fig. 6a). Raman spectroscopy was performed on I_2-free and I_2-based polymer electrolytes (Fig. 6b). The peak at 112 cm^{-1} for I_2-based polymer electrolyte, confirms the complete conversion of I^- to I_3^- (symmetric stretching vibration) with the addition of I_2 [50]. Whereas, the weaker band between 135 and 155 cm^{-1} can be assigned to the asymmetric stretching mode of I_3^- and presence of polyiodides [50,51]. Generation of polyiodides in I_2-based electrolytes caused the recombination of holes and electrons as also confirmed by increased dark current in I_2 based DSSC shown in Fig. 5b.

Impedance spectroscopy (EIS) was used to examine the charge transfer process of DSSCs in dark under open circuit voltage conditions [29]. The Nyquist and Bode phase plots of the DSSCs comprising the liquid and polymer electrolytes are shown in Fig. 7a and b, respectively. Three signatures can be identified in the EIS spectrum in the studied frequency range (0.1 Hz to 300 kHz). The first (high frequency) and second (middle frequency) semicircles correspond to the charge-transfer resistances at the counter electrode (R_1) and electrolyte–TiO_2 interfaces (R_2), while the third one (R_3) in the lower frequency range corresponds to the diffusion resistance of the electrolyte [52]. The circuit used to fit the data is presented in the insert of Fig. 7a and the corresponding values are briefed in Table 3. The sheet resistance (R_s) comprises of the contacts/wires and electrolyte resistance. The higher R_s value of I_2-free ImI-PDMS/EC-based device can be explained for the low FF [32,53]. The lower value of R_1 and R_2 for the ImI-PDMS/EC-based device confirms the superior catalytic activity of I_2-free electrolyte at the counter electrode and lower recombination leading to enhanced V_{oc}, respectively.

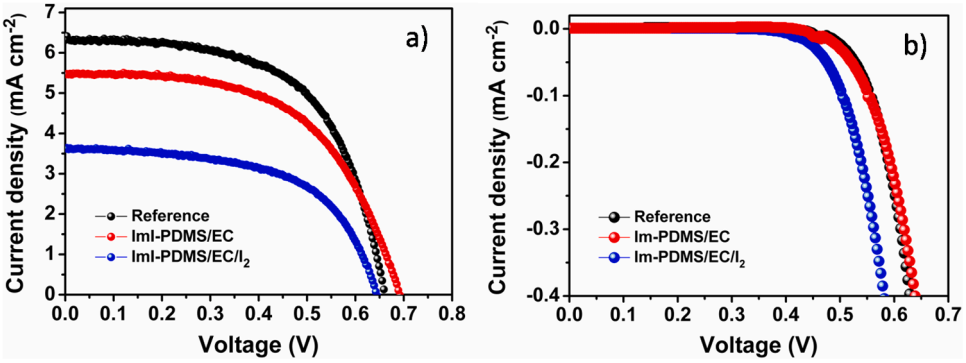

Fig. 5. *J-V* curves of devices using polymer and liquid-state electrolytes; (a) ~ 0.6 sun illumination, and (b) in dark conditions.

Table 2
Photovoltaic parameters of DSSCs based on TiO_2 NTs and various electrolytes.

DSSC	V_{oc} (V)	J_{sc} (mA cm^{-2})	FF	PCE (%)
Reference	0.66	6.33	0.60	4.15
ImI-PDMS/EC/I_2	0.64	3.63	0.58	2.30
ImI-PDMS/EC	0.69	5.48	0.56	3.55

However, the extremely large R_3 value of the I_2-free ImI-PDMS/EC-based device shows the highly insufficient amount of I_3^- ions as the EIS measurements were done in dark conditions.

Then again, the effective lifetime of electrons (τ_e) can be estimated from the maximum frequency (f_{max}) in the middle frequency range related to the charge transfer reaction at the TiO_2 NT/electrolyte interface by the following Eq. (1) [54].

$$\tau_e = \frac{1}{2_{JI} f_{max}} \quad (1)$$

As shown in Table 4, I_2-free ImI-PDMS/EC-based device shows the highest electron lifetime (67.8 ms) followed by the liquid electrolyte (45.4 ms) and ImI-PDMS/EC/I_2 (42.9 ms) based devices.

The open-circuit voltage decay (OCVD) measurement was performed by illuminating the device in open circuit condition and then observing the voltage decay as carriers recombine when the illumination is turned off [55,56]. The devices were illuminated by driving the white LED with square wave pulses. The LED input and solar cell output were synchronized and recorded by the oscilloscope. Fig. 8a-b represent the OCVD experimental setup and schematic representation measured for the I_2-free and I_2-based polymer electrolytes based devices, respectively. Upon turning off the illumination, the charge recombination at the interface results in a decrease of V_{oc}. The longer the V_{oc} decay time the slower is the charge recombination[35]. From Fig. 8c, it is found that the decay time for I_2-free devices was longer than that of the I_2-based and

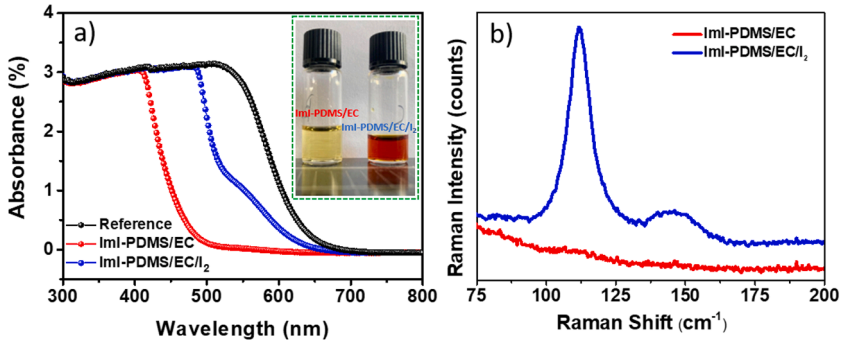

Fig. 6. a) UV–visible absorption and b) Raman spectra of the different electrolytes investigated.

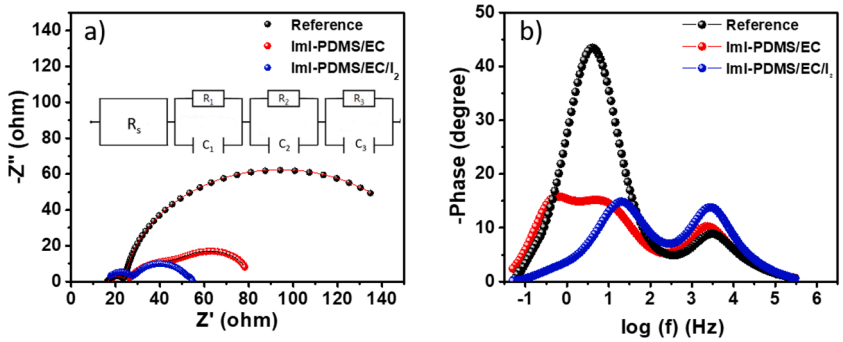

Fig. 7. (a) Nyquist plots and (b) Bode phase plots measured in dark conditions at an V_{oc} bias for DSSCs using the different electrolytes. Insert in Fig. 7a shows the corresponding equivalent circuit.

Table 3
Values of the circuit elements obtained by the EIS data fitting.

Sample code	R_s (Ω)	R_1(Ω)	R_2 (Ω)	R_3 (Ω)	f_{max} (Hz)	τ_e (ms)
Reference	16.5	4.5	14.7	2.3	3.51	45.4
ImI-PDMS/EC/I_2	16.3	11.3	25.3	2.0	3.71	42.9
ImI-PDMS/EC	17.6	8.9	24.0	30.5	2.35	67.8

found to be in good agreement with the device performances and impedance spectroscopy results. The electron lifetime could be correlated with the V_{oc} decay rate through the following equation 2:

$$\tau_e = -\frac{k_B T}{q} \Big/ \left(\frac{dV_{oc}}{dt}\right) \quad (2)$$

Where k_B is the Boltzmann constant, T is the room temperature in *kelvin*, q is the elementary charge and t is the time. As shown in Fig. 8d, the I_2-free devices have a longer electron lifetime than that of I_2-based ones, clearly showing the advantages of omitting I_2 from the polymer for reducing the charge recombination.

3.4. Long term stability

Fig. 9a shows the accelerated ageing test of the devices with the polymer (ImI-PDMS/EC and ImI-PDMS/EC/I_2) electrolytes versus the liquid electrolyte. The solar cell efficiency was measured at different time after keeping the devices under 1 sun conditions at 50 °C. It was noted that the DSSCs including ImI-PDMS/EC and ImI-PDMS/EC/I_2 exhibit excellent durability over 500 h, retaining up to 87% and 80% respectively of their initial efficiency, as opposed to the liquid-state DSSC which only retains 38%. The DSSCs with polymer electrolytes show a slight efficiency improvement initially, presumably due to the temperature increase which improved the conductivity (Fig. 2b). The I_2-free DSSC displayed prolonged at-rest stability due to the reduction of the I_3^--related corrosion and electrolyte leakage. Fig. 9b shows the at-rest stability of the replica ss-DSSCs with and without I_2 measured for several days under ambient conditions. It is noted that the DSSCs with no I_2 display superior stability measured over 150 days as compared to the DSSCs that contained I_2.

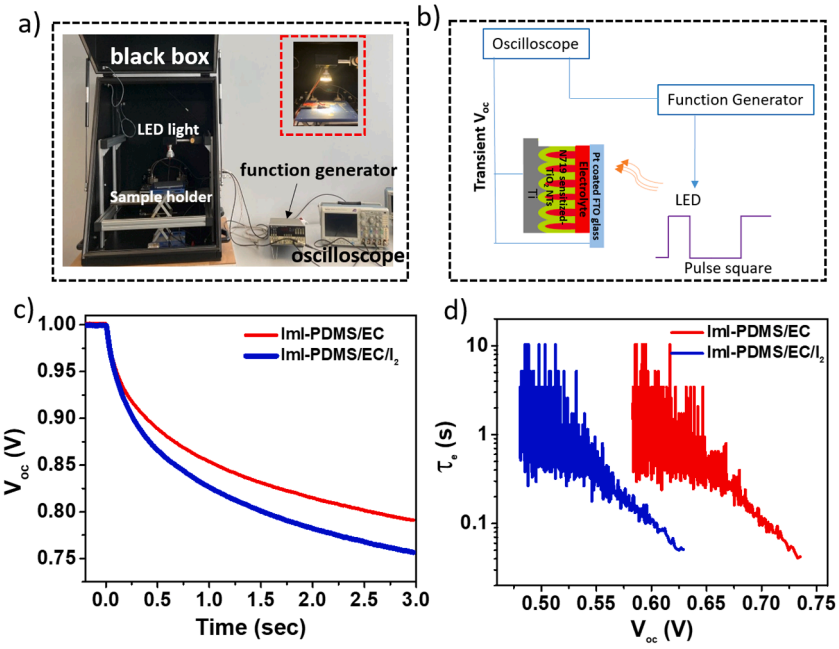

Fig. 8. (a) Experimental set-up and (b) schematic representations of the open-circuit voltage-decay (OCVD) measurement; (c) V_{oc} decay for ss-DSSCs based on ImI-PDMS/EC and ImI-PDMS/EC/I_2 electrolytes; (d) the electron lifetime derived from equation 2.

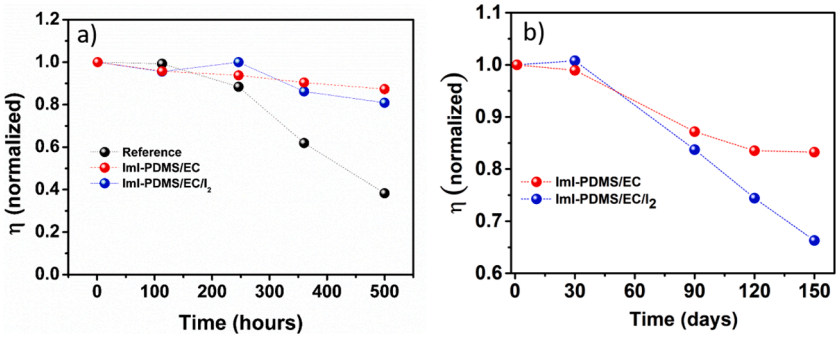

Fig. 9. Evolution of the normalized efficiency for the DSSCs using different electrolytes during accelerated aging tests at (a) under 1 sun and 50 °C and (b) under ambient conditions.

4. Conclusion

An I_2-free polysiloxane based polymer electrolyte was employed for the first time in combination with flexible 1D TiO_2 NT photoanodes in DSSC devices. Without the addition of I_2, the fabricated ss-DSSC with polymer electrolyte achieved a PCE of 3.55%, about 1.5 times higher compared to the device with I_2-based polymer electrolyte. Both V_{oc} and J_{sc} were notably improved when using the I_2-free polymer electrolytes as a result of the reduced charge recombination. The EIS and OCVD measurements further confirm that the I_2-free DSSCs have lower recombination losses and higher electron lifetime. Additionally, I_2-free DSSCs showed an improved stability compared to I_2-based DSSCs under accelerated and ambient conditions. Furthermore, the present I_2-free polymer electrolytes coupled with the TiO_2 NT photoanodes increase the visible light absorption and demonstrate effective pore infiltration paving the way towards the fabrication of flexible DSSCs. Further optimization of the DSSCs with various photoanodes and I_2-free polymer electrolytes is actually in progress.

Declaration of Competing Interest

None

Acknowledgements

The centre of Excellence of Multifunctional Architectured Materials "CEMAM" n° AN-10-LABX-44–01, the ARC 4 Énergies-Région Rhône-Alpes and the IDS FunMAT-International Doctorate School in Functional Materials are acknowledged by the authors for financial support. The authors are indebted to Mr Bruno Flament and Dr. Lionel Hirsch (University of Bordeaux, IMS UMR 5218 CNRS) for IPCE measurements.

Supplementary materials

Supplementary material associated with this article can be found, in the online version, at doi:10.1016/j.apsadv.2021.100120.

References

[1] M.A. Green, E.D. Dunlop, J. Hohl-Ebinger, M. Yoshita, N. Kopidakis, X. Hao, Solar cell efficiency tables (version 56), Prog. Photovolt. Res. Appl. 28 (2020) 629–638.
[2] A. Hagfeldt, G. Boschloo, L. Sun, L. Kloo, H. Pettersson, Dye-sensitized solar cells, Chem. Rev. 110 (2010) 6595–6663.
[3] B. O'Rdgan, M. Gratzel, A low-cost high-efficiency solar cell based on dye-sensitized colloidal TiO2, Nature 353 (1991) 737–739.
[4] Y. Cao, Y. Liu, S.M. Zakeeruddin, A. Hagfeldt, M. Grätzel, Direct contact of selective charge extraction layers enables high-efficiency molecular photovoltaics, Joule 2 (2018) 1108–1117.
[5] M. Kokkonen, P. Talebi, J. Zhou, S. Asgari, S.A. Soomro, F. Elsehrawy, J. Halme, S. Ahmad, A. Hagfeldt, S.G. Hashmi, Advanced research trends in dye-sensitized solar cells, J. Mater. Chem. A. (2021).
[6] D. Devadiga, M. Selvakumar, P. Shetty, M.S. Santosh, Recent progress in dye sensitized solar cell materials and photo-supercapacitors: a review, J. Power Sources. 493 (2021), 229698.
[7] K. Kakiage, Y. Aoyama, T. Yano, K. Oya, J. Fujisawa, M. Hanaya, Highly-efficient dye-sensitized solar cells with collaborative sensitization by silyl-anchor and carboxy-anchor dyes, Chem. Commun. 51 (2015) 15894–15897.
[8] P. Agarwala, D. Kabra, A review on triphenylamine (TPA) based organic hole transport materials (HTMs) for dye sensitized solar cells (DSSCs) and perovskite solar cells (PSCs): evolution and molecular engineering, J. Mater. Chem. A. 5 (2017) 1348–1373.
[9] A.F. Nogueira, C. Longo, M.-.A. De Paoli, Polymers in dye sensitized solar cells: overview and perspectives, Coord. Chem. Rev. 248 (2004) 1455–1468.
[10] B. O'Regan, F. Lenzmann, R. Muis, J. Wienke, A solid-state dye-sensitized solar cell fabricated with pressure-treated P25-TiO2 and CuSCN: analysis of pore filling and IV characteristics, Chem. Mater. 14 (2002) 5023–5029.
[11] C. Zafer, K. Ocakoglu, C. Ozsoy, S. Icli, Dicationic bis-imidazolium molten salts for efficient dye sensitized solar cells: synthesis and photovoltaic properties, Electrochim. Acta 54 (2009) 5709–5714.
[12] T. Stergiopoulos, I.M. Arabatzis, G. Katsaros, P. Falaras, Binary polyethylene oxide/titania solid-state redox electrolyte for highly efficient nanocrystalline TiO2 photoelectrochemical cells, Nano Lett. 2 (2002) 1259–1261.
[13] Y. Kim, Y.-.E. Sung, J.-.B. Xia, M. Lira-Cantu, N. Masaki, S. Yanagida, Solid-state dye-sensitized TiO 2 solar cells using poly (3, 4-ethylenedioxythiophene) as substitutes of iodine/iodide electrolytes and noble metal catalysts on FTO counter electrodes, J. Photochem. Photobiol. Chem. 193 (2008) 77–80.
[14] J.N. de Freitas, A.F. Nogueira, M.-.A. De Paoli, New insights into dye-sensitized solar cells with polymer electrolytes, J. Mater. Chem. 19 (2009) 5279–5294.
[15] T. Bandara, M. Dissanayake, W. Jayasundara, I. Albinsson, B.-.E. Mellander, Efficiency enhancement in dye sensitized solar cells using gel polymer electrolytes based on a tetrahexylammonium iodide and MgI 2 binary iodide system, Phys. Chem. Chem. Phys. 14 (2012) 8620–8627.
[16] Y. Wang, Recent research progress on polymer electrolytes for dye-sensitized solar cells, Sol. Energy Mater. Sol. Cells. 93 (2009) 1167–1175.
[17] G.L. De Gregorio, R. Agosta, R. Giannuzzi, F. Martina, L. De Marco, M. Manca, G. Gigli, Highly stable gel electrolytes for dye solar cells based on chemically engineered polymethacrylic hosts, Chem. Commun. 48 (2012) 3109–3111.
[18] M.S. Su'ait, M.Y.A. Rahman, A. Ahmad, Review on polymer electrolyte in dye-sensitized solar cells (DSSCs), Sol. Energy. 115 (2015) 452–470.
[19] W. Zhang, Y. Wu, H.W. Bahng, Y. Cao, C. Yi, Y. Saygili, J. Luo, Y. Liu, L. Kavan, J.-.E. Moser, Comprehensive control of voltage loss enables 11.7% efficient solid-state dye-sensitized solar cells, Energy Environ. Sci. 11 (2018) 1779–1787.
[20] C. Zhang, S. Gamble, D. Ainsworth, A.M. Slawin, Y.G. Andreev, P.G. Bruce, Alkali metal crystalline polymer electrolytes, Nat. Mater. 8 (2009) 580–584.
[21] H.-.W. Pang, H.-.F. Yu, Y.-.J. Huang, C.-.T. Li, K.-.C. Ho, Electrospun membranes of imidazole-grafted PVDF-HFP polymeric ionic liquids for highly efficient quasi-solid-state dye-sensitized solar cells, J. Mater. Chem. A. 6 (2018) 14215–14223.
[22] G. Wang, C. Yan, J. Zhang, S. Hou, W. Zhang, Highly efficient solid-state dye-sensitized solar cells based on hexylimidazolium iodide ionic polymer electrolyte prepared by in situ low-temperature polymerization, J. Power Sources. 345 (2017) 131–136.
[23] M. Thomas, S. Rajiv, Grafted PEO polymeric ionic liquid nanocomposite electrospun membrane for efficient and stable dye sensitized solar cell, Electrochim. Acta 341 (2020), 136040.
[24] F.-.S. Lin, M. Sakthivel, M.-.S. Fan, J.-.J. Lin, R.-.J. Jeng, K.-.C. Ho, A novel multifunctional polymer ionic liquid as an additive in iodide electrolyte combined with silver mirror coating counter electrodes for quasi-solid-state dye-sensitized solar cells, J. Mater. Chem. A. 9 (2021) 4907–4921.
[25] A.K. Bharwal, N.A. Nguyen, C. Iojoiu, C. Henrist, F. Alloin, New polysiloxane bearing imidazolium iodide side chain as electrolyte for photoelectrochemical cell, Solid State Ion. 307 (2017) 6–13. https://doi.org/10.1016/j.ssi.2017.05.004.
[26] G.L. De Gregorio, R. Giannuzzi, M.P. Cipolla, R. Agosta, R. Grisorio, A. Capodilupo, G.P. Suranna, G. Gigli, M. Manca, Iodopropyl-branched polysiloxane gel electrolytes with improved ionic conductivity upon cross-linking, Chem. Commun. 50 (2014) 13904–13906.
[27] M.P. Cipolla, G.L. De Gregorio, R. Grisorio, R. Giannuzzi, G. Gigli, G.P. Suranna, M. Manca, An ion conductive polysiloxane as effective gel electrolyte for long stable dye solar cells, J. Power Sources. 356 (2017) 191–199.
[28] A.K. Bharwal, L. Manceriu, F. Alloin, C. Iojoiu, J. Dewalque, T. Toupance, C. Henrist, Tuning bimodal porosity in TiO2 photoanodes towards efficient solid-state dye-sensitized solar cells comprising polysiloxane-based polymer electrolyte, Microporous Mesoporous Mater 273 (2019) 226–234.
[29] A.K. Bharwal, L. Manceriu, C. Iojoiu, J. Dewalque, T. Toupance, L. Hirsch, C. Henrist, F. Alloin, Ionic-Liquid-like Polysiloxane Electrolytes for Highly Stable Solid-State Dye-Sensitized Solar Cells, ACS Appl. Energy Mater. 1 (2018) 4106–4114, https://doi.org/10.1021/acsaem.8b00769.
[30] A.K. Bharwal, L. Manceriu, F. Alloin, C. Iojoiu, J. Dewalque, T. Toupance, C. Henrist, Bimodal titanium oxide photoelectrodes with tuned porosity for improved light harvesting and polysiloxane-based polymer electrolyte infiltration, Sol. Energy. 178 (2019) 98–107.
[31] G. Wang, L. Wang, S. Zhuo, S. Fang, Y. Lin, An iodine-free electrolyte based on ionic liquid polymers for all-solid-state dye-sensitized solar cells, Chem. Commun. 47 (2011) 2700–2702.
[32] W.-.C. Yu, L.-.Y. Lin, W.-.C. Chang, S.-.H. Zhong, C.-.C. Su, Iodine-free nanocomposite gel electrolytes for quasi-solid-state dye-sensitized solar cells, J. Power Sources. 403 (2018) 157–166.
[33] Y. Rong, X. Li, G. Liu, H. Wang, Z. Ku, M. Xu, L. Liu, M. Hu, Y. Yang, M. Zhang, Monolithic quasi-solid-state dye-sensitized solar cells based on iodine-free polymer gel electrolyte, J. Power Sources 235 (2013) 243–250.
[34] Y. Rong, Z. Ku, M. Xu, L. Liu, M. Hu, Y. Yang, J. Chen, A. Mei, T. Liu, H. Han, Efficient monolithic quasi-solid-state dye-sensitized solar cells based on poly (ionic liquids) and carbon counter electrodes, RSC Adv. 4 (2014) 9271–9274.
[35] Z. Yu, S. You, C. Wang, C. Bu, S. Bai, Z. Zhou, Q. Tai, W. Liu, S. Guo, X. Zhao, Efficient dye-sensitized solar cells employing highly environmentally-friendly ubiquinone 10 based I 2-free electrolyte inspired by photosynthesis, J. Mater. Chem. A. 2 (2014) 9007–9010.
[36] D.A. Chalkias, C. Charalampopoulos, A.K. Andreopoulou, A. Karavioti, E. Stathatos, Spectral engineering of semi-transparent dye-sensitized solar cells using new triphenylamine-based dyes and an iodine-free electrolyte for greenhouse-oriented applications, J. Power Sources 496 (2021), 229842.
[37] M. Ye, X. Xin, C. Lin, Z. Lin, High efficiency dye-sensitized solar cells based on hierarchically structured nanotubes, Nano Lett. 11 (2011) 3214–3220.
[38] S. So, I. Hwang, J. Yoo, S. Mohajernia, M. Mačković, E. Spiecker, G. Cha, A. Mazare, P. Schmuki, Inducing a Nanotwinned Grain Structure within the TiO2 Nanotubes Provides Enhanced Electron Transport and DSSC Efficiencies>10%, Adv. Energy Mater. 8 (2018), 1800981.
[39] J.R. Jennings, A. Ghicov, L.M. Peter, P. Schmuki, A.B. Walker, Dye-sensitized solar cells based on oriented TiO2 nanotube arrays: transport, trapping, and transfer of electrons, J. Am. Chem. Soc. 130 (2008) 13364–13372.

[40] P. Roy, D. Kim, K. Lee, E. Spiecker, P. Schmuki, TiO2 nanotubes and their application in dye-sensitized solar cells, Nanoscale 2 (2010) 45–59.
[41] T. Stergiopoulos, E. Rozi, R. Hahn, P. Schmuki, P. Falaras, Enhanced Open-Circuit Photopotential in Quasi-Solid-State Dye-Sensitized Solar Cells Based on Polymer Redox Electrolytes Filled with Anodic Titania Nanotubes, Adv. Energy Mater. 1 (2011) 569–572.
[42] S. So, I. Hwang, P. Schmuki, Hierarchical DSSC structures based on "single walled" TiO 2 nanotube arrays reach a back-side illumination solar light conversion efficiency of 8%, Energy Environ. Sci. 8 (2015) 849–854.
[43] Z. Seidalilir, R. Malekfar, H.-.P. Wu, J.-.W. Shiu, E.W.-G. Diau, High-Performance and Stable Gel-State Dye-Sensitized Solar Cells Using Anodic TiO2 Nanotube Arrays and Polymer-Based Gel Electrolytes, ACS Appl. Mater. Interfaces. 7 (2015) 12731–12739.
[44] Y. Liu, Y. Cheng, K. Chen, G. Yang, Z. Peng, Q. Bao, R. Wang, W. Chen, Enhanced light-harvesting of the conical TiO2 nanotube arrays used as the photoanodes in flexible dye-sensitized solar cells, Electrochim. Acta 146 (2014) 838–844.
[45] D.N. Joshi, R.A. Prasath, Low temperature rapid synthesis of direct mesoporous anatase TiO2nano-aggregates and its application in dye-sensitized solar cell, Mater. Today Proc. 3 (2016) 2413–2421.
[46] D.N. Joshi, S. Sudhakar, R.V. Nair, R.A. Prasath, Swift sol–gel synthesis of mesoporous anatase-rich TiO 2 aggregates via microwave and a lyophilization approach for improved light scattering in DSSCs, J. Mater. Sci. 52 (2017) 2308–2318.
[47] H.-.Y. Yang, W.-.Y. Rho, S.K. Lee, S.H. Kim, Y.-.B. Hahn, TiO2 nanoparticles/nanotubes for efficient light harvesting in perovskite solar cells, Nanomaterials 9 (2019) 326.
[48] S.-.J. Seo, K.A. Bialecka, M.-.S. Kang, A. Hinsch, S.-.H. Moon, In-situ analyses of triiodide formation in an iodine-free electrolyte for dye-sensitized solar cells using electro-diffuse-reflection spectroscopy (EDRS), J. Power Sources 275 (2015) 675–680.
[49] A. Agresti, S. Pescetelli, E. Gatto, M. Venanzi, A. Di Carlo, Polyiodides formation in solvent based Dye Sensitized Solar Cells under reverse bias stress, J. Power Sources. 287 (2015) 87–95.
[50] E. Tanaka, N. Robertson, Polyiodide solid-state dye-sensitized solar cell produced from a standard liquid I-/I 3- electrolyte, J. Mater. Chem. A. 8 (2020) 19991–19999.
[51] M.I. Asghar, J. Halme, S. Kaukonen, N. Humalamäki, P. Lund, J. Korppi-Tommola, Intriguing photochemistry of the additives in the dye-sensitized solar cells, J. Phys. Chem. C. 120 (2016) 27768–27781.
[52] F. Fabregat-Santiago, G. Garcia-Belmonte, I. Mora-Sero, J. Bisquert, Characterization of nanostructured hybrid and organic solar cells by impedance spectroscopy, Phys. Chem. Chem. Phys. 13 (2011) 9083–9118.
[53] M. Cheng, X. Yang, S. Li, X. Wang, L. Sun, Efficient dye-sensitized solar cells based on an iodine-free electrolyte using L-cysteine/L-cystine as a redox couple, Energy Environ. Sci. 5 (2012) 6290–6293.
[54] C. Shi, L. Qiu, X. Chen, H. Zhang, L. Wang, F. Yan, Silica Nanoparticle Doped Organic Ionic Plastic Crystal Electrolytes for Highly Efficient Solid-State Dye-Sensitized Solar Cells, ACS Appl. Mater. Interfaces. 5 (2013) 1453–1459, https://doi.org/10.1021/am302925s.
[55] A. Zaban, M. Greenshtein, J. Bisquert, Determination of the electron lifetime in nanocrystalline dye solar cells by open-circuit voltage decay measurements, ChemPhysChem 4 (2003) 859–864.
[56] P. Perkhun, W. Köntges, F. Pourcin, D. Esteoulle, E. Barulina, N. Yoshimoto, P. Pierron, O. Margeat, C. Videlot-Ackermann, A.K. Bharwal, High-Efficiency Digital Inkjet-Printed Non-Fullerene Polymer Blends Using Non-Halogenated Solvents, Adv. Energy Sustain. Res. 2 (2021), 2000086.